Pharm Res (2011) 28:2403–2411
DOI 10.1007/s11095-011-0456-z

# Intact Nanoparticulate Indomethacin in Fast-Dissolving Carrier Particles by Combined Wet Milling and Aerosol Flow Reactor Methods

Timo Laaksonen • Peng Liu • Antti Rahikkala • Leena Peltonen • Esko I. Kauppinen • Jouni Hirvonen • Kristiina Järvinen • Janne Raula

Received: 4 March 2011 / Accepted: 20 April 2011 / Published online: 4 May 2011


## ABSTRACT

***Purpose*** Drug development is often hindered by a drug's low dissolution rate. We present a method to increase dissolution rate of a drug powder by producing crystalline nanoparticles that are dispersed in carrier microparticles.

***Methods*** Indomethacin crystals of a few hundred nanometers are prepared by media milling using poloxamer 188 as a stabilizer. Nanoparticles are embedded into microparticles with a mannitol matrix and an L-leucine coating layer using an aerosol flow reactor method.

***Results*** Microparticles stabilize the primary nanoparticles in an intact crystalline form and release them when re-dispersed in aqueous medium. Secondary microparticle structure dissolves rapidly, resulting in a fast release and dissolution of indomethacin. In this manner, it is possible to change the surface layer of the particles from the one needed for nanoparticle production to one more suitable for process formulation of pharmaceuticals for, *e.g.,* tablet or pulmonary products.

***Conclusions*** Particle assemblies where nano-sized crystalline drug domains are embedded in solid microparticles are presented. The present work is a promising approach towards a "nanos-in-micros" concept as a tool for pharmaceutical nanoparticle processing.

**KEY WORDS** aerosol flow reactor · drug dissolution · media milling · microparticles · nanoparticles

## INTRODUCTION

Drug development is often hindered by a slow dissolution of the new drug compounds. Material solubility and dissolution rate increase notably when particles are in the nanometer size range, which is very beneficial especially for poorly soluble drugs (1). Nanocrystallization is one promising technique to improve the dissolution rate of poorly soluble drug materials (2,3), but the main problem with the produced nanopowders is the production of the final formulation from the nanocrystalline material. To maintain the benefits of nanosized materials, but in order to avoid the problems related to the small size, *e.g.* cohesion, poor flowability, and aggregation tendency, nanoparticles can be further formulated into micron-sized particles. Further, the nanoparticles can be partly amorphous or coated with amorphous or sticky stabilizers such as surfactants or low-molecular-weight polymers. This, in addition to their size, makes their handling very difficult.

T. Laaksonen (✉) • P. Liu • L. Peltonen • J. Hirvonen
Division of Pharmaceutical Technology, Faculty of Pharmacy
University of Helsinki
P.O. Box 56, 00014 Helsinki, Finland
e-mail: timo.laaksonen@helsinki.fi

A. Rahikkala • E. I. Kauppinen • J. Raula (✉)
Department of Applied Physics Aalto University School of Science
P.O. Box 15100, 00076 Aalto, Finland
e-mail: janne.raula@tkk.fi

K. Järvinen
School of Pharmacy, Faculty of Health Sciences
University of Eastern Finland
70211 Kuopio, Finland

When formulated into microparticles, the surface layer of the final carrier particles can be reconstructed with a completely different material. A crystalline hydrophilic coating would be easier for powder handling than a sticky amorphous layer. The possibility to further tailor this secondary surface is also a challenge.

Spray-drying and freeze-drying have been used to form nanostructured microparticles by drying the suspensions of previously prepared nanomaterials such as nanocapsules, porous nanomaterials, nanoparticles, solid lipid nanoparticles, nanocrystals, *etc.* (4–10). Consolidation of nanomaterials into microparticles improves the handling of powder wherein the properties of the original nanomaterials are retained. Often, some matrix-forming agents, such as mannitol, lactose, or trehalose, have been used to form the bulk in which the nanoparticles are homogenously dispersed (11,12). However, the use of such relatively hygroscopic excipients may render the particles physically and chemically unstable if the excipient is amorphous or the particles are not protected against humidity. Moreover, the amorphous form is prone to uncontrolled crystallization upon storage, resulting not only in particle sintering (13) but also possible changes in drug polymorphism that may affect drug dosing and bioavailability (14). All these are serious concerns with particles less than 10 μm but in particular with submicron particles. Many of the above-mentioned techniques produce cohesive (large particle contact area), electrostatic, or low density powders, which can cause them to fail in an accurate dosing. Apart from spray-drying, the other techniques involve several steps to produce the final powder, which is not cost and time effective. When prepared by spray-drying, the materials in the particles are commonly amorphous due to very rapid drying of particles. Neither spray-drying nor freeze-drying enable the fabrication of coating layers onto nanostructured microparticles with different functionalities in a single step.

A recently introduced aerosol flow reactor method is based on the controlled drying rate of particles and the conversion of droplets to particles in a laminar flow (13,15). The method is a single-step, continuous process where a control over the drying rate of droplets allows molecular arrangements to take place within the droplets prior to particle drying. For instance, surface-active compounds accumulate at the water-gas interface of droplets, thus encapsulating the particles. Moreover, the drug particles can be coated by physical vapor deposition (PVD) directly in the gas-phase. Leucine compounds as surface-modifying materials have shown to improve flowability and dispersibility of powders (16–19). In our earlier studies we used PVD to encapsulate the drug particles with an amino acid L-leucine (20–23). The inner encapsulating layer protected the drug salbutamol sulphate against humidity, whereas the outer rough and crystalline coating layer provided excellent aerosolization properties by lowering the adhesion forces between the particles (24,25). For instance, the dosing of the coated particles from a breath-actuated inhaler was possible without coarse carrier particles conventionally used in commercial inhalation products. The PVD coatings by the aerosol method can be applied to diverse solid particles of different size, shape, and crystalline state.

The drug nanoparticles as such are almost impossible to handle efficiently in pharmaceutical formulation processes. It is proposed that embedding these primary drug nanoparticles in a carrier matrix can provide stable powder formulations suitable, for instance, for inhalation products or automated tablet manufacturing. In the present work, the goal was to encapsulate fast-dissolving drug nanocrystals into carrier microparticles while retaining the dissolution rate benefits of the initial particles. Fig. 1 illustrates this "nanos-in-micros" concept and function of the particle assembly.

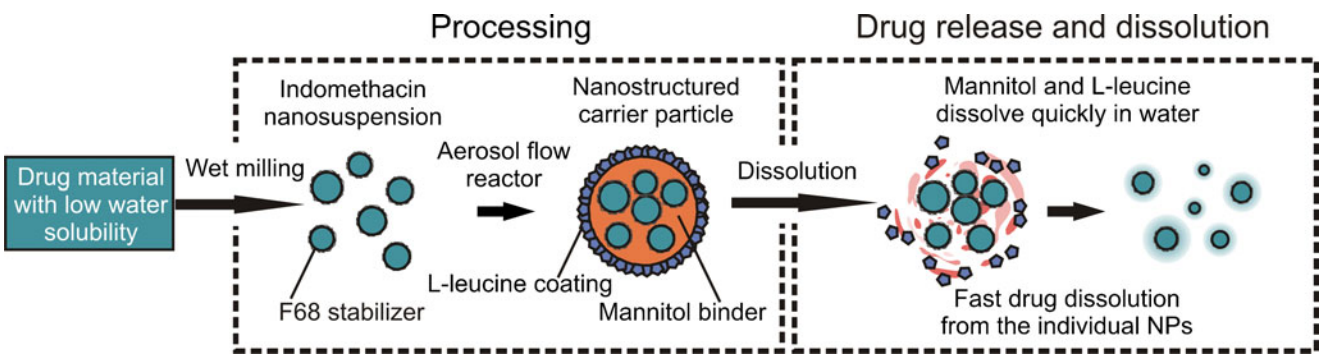


**Fig. 1** Illustration of the concept for producing and using nanostructured microparticles. Wet-milled nanosuspensions are dried and embedded into a mannitol matrix and coated with a crystalline L-leucine layer in an aerosol flow reactor. Microparticle structure dissolves rapidly in water, and primary nanoparticles are released. Fast drug dissolution is due to the small size of the initial particles.

## MATERIALS AND METHODS

### Materials

All chemicals were obtained from standard sources and were used without further purification.

### Nanoparticle Production by Wet Media Milling

The initial nanosuspensions were prepared using a wet-milling technique with Poloxamer 188 (Lutrol® F68, BASF Co.) as a stabilizing polymer. F68 (500 mg) was dissolved in water (5 ml). Indomethacin (IND, 2 g) powder was dispersed in the aqueous stabilizer solution. These parameters are based on extensive testing done with indomethacin and different stabilizers (26). The suspensions were pipetted into the milling bowl containing of milling pearls (70 g, zirconium oxide, diameter 1 mm). Additional water (5 ml) was used to collect the residual suspensions from the beaker to the milling bowl. The milling bowl was placed in a planetary ball mill (Pulverisette 7 Premium, Fritsch Co., Germany), and grinding was performed at 1100 rpm. A total grinding time of 30 min was done in ten 3-min grinding cycles. After each grinding cycle there was a 15 min pause in order to cool down the milling vessel. After the milling, the nanosuspensions were separated from the grinding pearls by sieving.

### Aerosol Flow Reactor (AFR) Method

The resulting indomethacin nanosuspensions were diluted ca. 40-fold with deionized water. This resulted in ca. 5 g/l drug suspensions. Mannitol (Alfa Aesar) 20 g/l and L-leucine (Alfa Aesar) 10 g/l were dissolved in the diluted nanosuspensions, resulting in precursor suspensions. The amounts were based on previous studies done with the method and should result in micron-sized particles with a crystalline L-leucine coating (18,22). Samples without mannitol and L-leucine were also prepared as controls. The dry, solid particles from the nanosuspensions were prepared using the aerosol flow reactor method as follows (13,15). The precursor suspensions were atomized using an air-jet atomizer (Collison atomizer, TSI model 3076) which was modified to produce also micron-sized droplets. In this atomizer, the opposing impaction wall was removed to allow large solute droplets to enter the aerosol reactor. Nitrogen gas was used to carry the particles through the tubular aerosol reactor in a laminar flow of 3 l/min. The total residence time of the aerosol in the reactor was 9 s. The temperature of the reactor was controlled with four separate heating blocks and monitored with five separate thermocouples inserted in the reactor. The blocks were heated for the two sets of temperature profiles in order from aerosol entry to exit: 100–100–100–100°C (AFR 100) and 100–100–100–160°C (AFR 160). The residence time of the aerosol in the zone at 160°C was 1.5 s. The dry particle aerosol was diluted (ratio of 1:10) in a porous tube diluter with nitrogen gas (20°C) before collecting size-exclusively with a Berner-type low-pressure impactor (BLPI) onto aluminum foils (27).

### Size and Size Distribution Measurements

The size and polydispersity index (PI) of nanosuspensions and dried powder were determined by photon correlation spectroscopy (PCS). Nanosuspensions were diluted, and dried powder was redispersed in saturated IND solution prior to measurement. After vortex shaking and sonication for 3 min, suspensions were diluted with saturated solution for size measurement. The tests were repeated in triplicate. Particle size distributions of the aerosols were measured from gas-phase at the aerosol reactor downstream using a TSI scanning mobility particle sizer (SMPS) equipped with a long differential mobility analyzer (DMA, TSI model 3081) and a condensation particle counter (CPC, TSI model 3022).

### Particle Morphology Studies

The nanosuspensions samples were pipetted on formvar film-coated copper grids with a mesh size 300 (Agar Scientific, Essex, UK) and dried at ambient conditions. The morphological evaluation of the particles in suspensions was performed by transmission electron microscopy (TEM, FEI Tecnai F12, Philips Electron optics, Holland). Dry particle morphology was studied with field-emission scanning electron microscopy (SEM, JEOL JSM-7500F, JEOL Ltd., Japan, acceleration voltage of 5 kV) and particle structure by cryo-TEM (JEOL JEM-3200FSC, JEOL Ltd., Japan, acceleration voltage of 300 kV).

### Drug Loading Determinations

The drug loading was measured for the size-separated samples after the aerosol process. A known amount of sample powder was taken and dissolved in ethanol:water solution (ethanol:water = 1:1, *v*/*v*). The sample solution was further diluted with the same solution prior to HPLC measurement. HPLC instrument (Agilent 1100 series, Agilent technologies, Germany) was used for quantification of the drug concentrations. Samples (20 μl) were injected into a Luna 3 μ C18 100A (150×4.6 mm) column (Phenomenex Co. California, USA). The mobile phase was acetonitrile and 0.2% phosphoric acid in water (pH 2.0) (60:40, *v*/*v*) and was used at a flow rate of 1.5 ml/min. The IND concentrations were quantified at a UV wavelength of 320 nm. Drug loading tests were done with a

Gemini NX column, flow rate of 1 ml/min and 65:35 acetonitrile:buffer ratio.

### Drug Release Tests

Dissolution behavior was studied for pure IND, physical mixtures, nanosuspensions and aerosol dried samples by paddle method according to the European Pharmacopoeia using a dissolution system Erweka DT-06 (Heusentamm, Germany). Phthalate buffer (pH = 5.0, 600 ml) at 37°C was used as the dissolution medium. A known amount of sample was transferred to the dissolution vessel and stirred at 100 rpm. Sink conditions were maintained during the dissolution test. At predetermined time intervals, a certain volume of dissolution media was withdrawn, and the same volume of fresh media was added. To remove any solid drug particles, samples were centrifuged at 13,000 rpm for 8 min. Drug concentrations were quantified by HPLC. The total IND amount in dissolution test was calculated using the formulation: The total IND amount = the sample weighted × drug loading.

### X-Ray Powder Diffraction (XRPD) Experiments

XRPD patterns were determined by an X-ray diffractometer (Bruker AXS D8, Karlsruhe, Germany). The XRPD was performed in symmetrical reflection mode using Cu-Kα radiation with $\lambda = 1.54$ Å (40 kV and 40 mA). The sample was placed on a flat aluminum sample holder. Data were collected by scanning from 5° to 40° with 0.02° steps, and the measuring time per step was 0.5 s.

### Differential Scanning Calorimeter (DSC) Experiments

Thermal properties were analyzed with a DSC 823e (Mettler Toledo Inc., Columbus, USA). The sample (4–9 mg) was placed in a sealed perforated aluminum pan. The temperature range for the measurement was from 25 to 310°C with the heating rate of 10°C/min. Measurements were performed under nitrogen flow of 50 ml/min. The data were analyzed with STARe software (Mettler Toledo, Columbus, USA).

## RESULTS AND DISCUSSION

The particle assemblies presented in Fig. 1 required a combination of two separate preparation procedures. First, wet media milling was used to make initial nanosuspensions composed of indomethacin nanocrystals. Second, these nanosuspensions were used as precursor suspensions to prepare solid carrier particles with the aerosol flow reactor (AFR) (Table I lists the composition of the suspensions). In the carrier particles, mannitol was used as a matrix material and L-leucine as the coating material.

### Particle Size, Morphology and Crystallinity

Figs. 2 and 3 show the SEM and TEM images of the particles, respectively. The melting points obtained from DSC are shown in Table II. The aerosol particles prepared from indomethacin nanosuspension without mannitol or L-leucine (AFR 100–1 and AFR 160–1) were physically unstable, *i.e.* particle integrity was not maintained in the collection, and the particles formed large agglomerates (Fig. 2c and d). It was assumed that F68 used as a stabilizer in the wet milling was mostly in an amorphous form in the aerosol particles. In this case the F68 was fluidic ($T_g = -63.4$°C) (28) at the collection temperature (25°C) that caused particle agglomeration. In addition, the partial melting of indomethacin ($T_m = 160$°C) in AFR 160–1 resulted in the re-crystallization of indomethacin upon the collection which is seen as large crystalline strips in Fig. 2d. Mannitol alone (AFR 100–2 and AFR 160–2) was not sufficient to stabilize particle integrity (Fig. 2e and f). Although the particles were stabilized with mannitol to some extent, the particles sintered when collected, especially in the case of AFR 160–2 sample (Fig. 2f). In addition to the fluidic nature of F68 and partial melting of indomethacin, this is due to the partial melting ($T_m = 166$°C) of mannitol in the aerosol reactor and subsequent re-crystallization upon the collection. With the L-leucine coating (AFR 100–3 and AFR 160–3), however, particle integrity was maintained, and non-sintered particles could be collected (Figs. 2a-b, g-h, 3). L-leucine is a surface-active material which diffuses to the surface of the droplets, thus forming a crystalline surface layer for the particles (29). In AFR 160–3 samples, a fraction of indomethacin melted and re-crystallized as needle-like crystals, which could be seen in the SEM and TEM images (Figs. 2h and 3c), whereas the major fraction of indomethacin was as original nanocrystals

**Table I** Precursor Solution Compositions for AFR and Dry Powder Sizes of the Prepared Powders. Sizes are Mass Mean Diameters

| | Precursor solution content (g/l) | | | | Powder size | |
|---|---|---|---|---|---|---|
| | F68 | Indomethacin | Mannitol | Leucine | Size (nm) | g.s.d. |
| AFR 100-1 | 1.25 | 5 | – | – | 956 | 1.7 |
| AFR 100-2 | 1.25 | 5 | 20 | – | 673 | 1.6 |
| AFR 100-3 | 1.25 | 5 | 20 | 10 | 824 | 1.5 |
| AFR 160-1 | 1.25 | 5 | – | – | 714 | 1.6 |
| AFR 160-2 | 1.25 | 5 | 20 | – | 665 | 1.6 |
| AFR 160-3 | 1.25 | 5 | 20 | 10 | 576 | 1.4 |

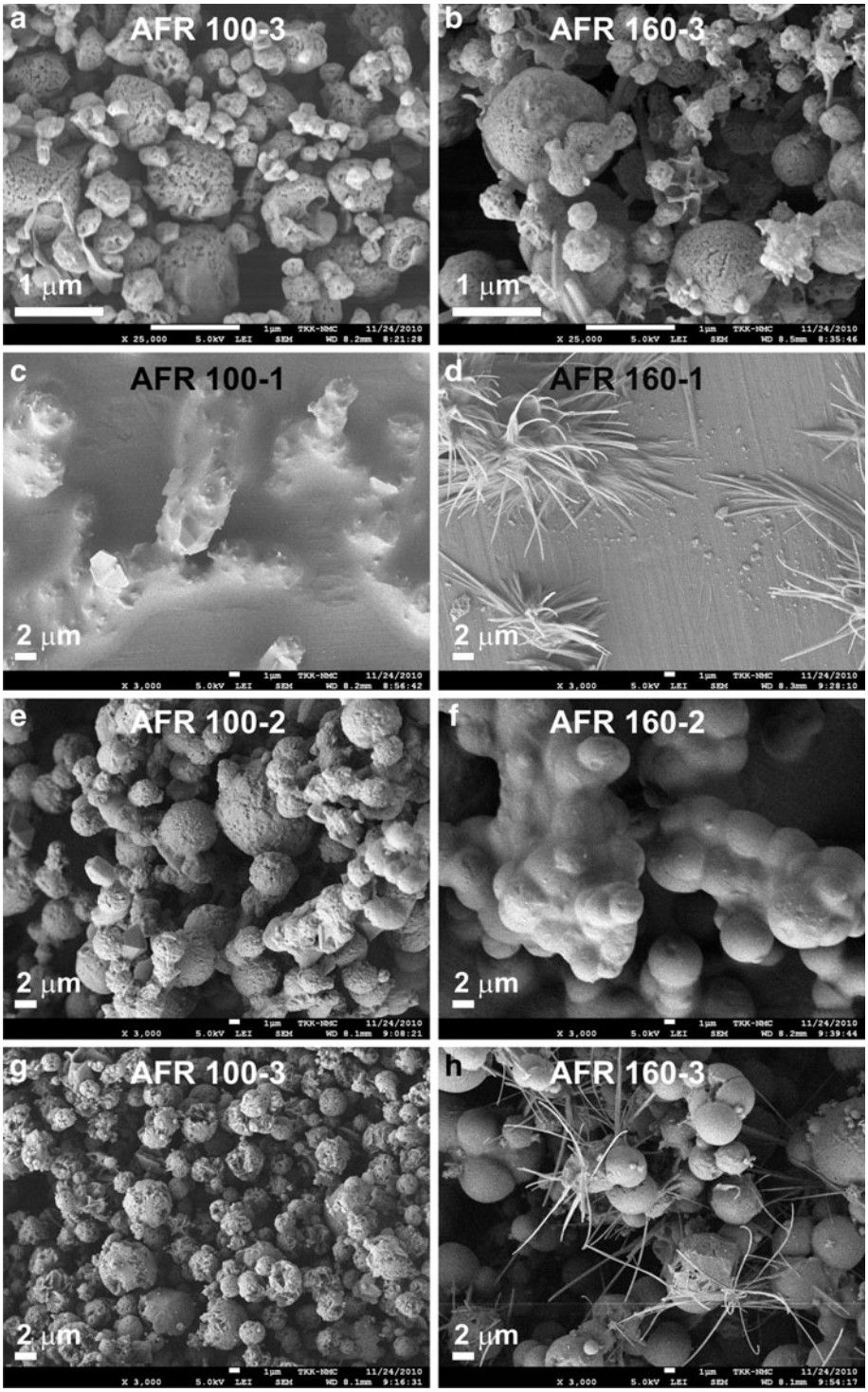


**Fig. 2** SEM images of aerosol flow reactor produced microparticles. Polydisperse samples: AFR 100–3 (**a**) and AFR 160–3 (**b**). Size-excluded samples with D50 of 3.9 $\mu$m: AFR 100–1 (**c**), AFR 100–2 (**e**), and AFR 100–1 (**g**) and AFR 160–2 (**d**), AFR 160–3 (**f**), and AFR 160–3 (**h**). Needle-like particles are indomethacin crystals after being melted and recrystallized in the aerosol process (**h**).

in the particle interiors. The AFR 100–3 sample did not have such separated indomethacin crystals, indicating that the indomethacin nanocrystalline domains in the microparticles were intact (Figs. 2d and 3b). These results highlight the importance of temperature control in the present particle preparation. Surprisingly, the molten state of the stabilizer F68 was not critical for the stability of carrier particles prepared with aerosol flow reactor.

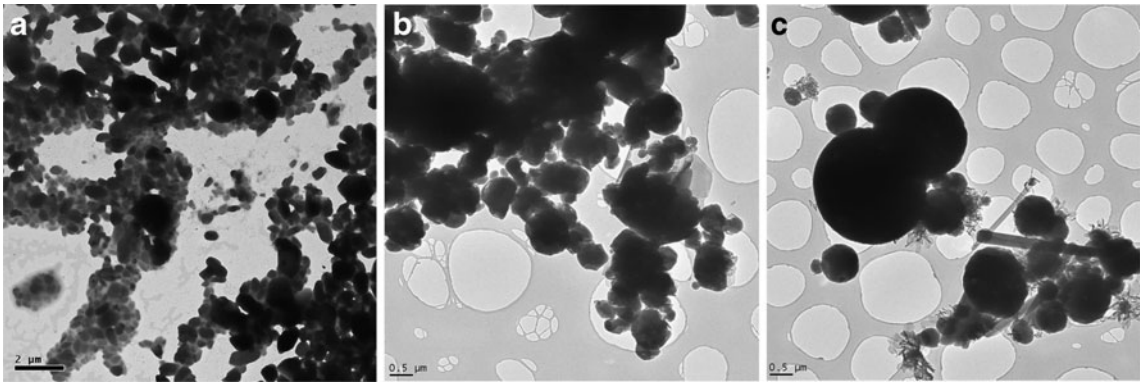


**Fig. 3** TEM images of (**a**) original indomethacin nanosuspensions with a 2 $\mu$m scale bar, (**b**) AFR 100–3 with a 0.5 $\mu$m scale bar, and (**c**) AFR 160–3 samples with a 0.5 $\mu$m scale bar. Recrystallized indomethacin can be seen in (**c**) as needle-like particles.

Powder X-ray diffraction results are shown in Fig. 4. Although quite complicated due to several components, XRPD peaks corresponding to crystalline mannitol, L-leucine and indomethacin could be assigned for AFR 100–3 and AFR 160–3 samples. The peaks for F68 were not detected, which could be due to the low amount in the samples (less than 3% of the sample mass), overlapping peaks with mannitol, or amorphous state in the samples. The melting points obtained from DSC results (Fig. 5) are shown in Table II. In the AFR 100–3 and AFR 160–3 samples, indomethacin melted at 10–20°C lower temperature than the bulk indomethacin. This lower melting point is comparable to the wet-milled indomethacin nanosuspensions before drying (Table II). DSC measurements of AFR 100–3 and AFR 160–3 samples did not indicate glass transition (42–47°C) or recrystallization of amorphous indomethacin (80–100°C) (30). Taken together, XRPD and DSC studies indicate that the crystallinity of indomethacin remained the same during the carrier particle production in both AFR 100 and AFR 160 samples, although in the latter samples indomethacin was partially melted and re-crystallized during the process. The melting

**Table II** The Onset Melting Temperature (°C) of DSC Peaks for F68, Bulk IND, Mannitol, L-leucine Measured for Bulk Materials and Aerosol Dried Samples

| | Melting temperature (°C) | | | |
|---|---|---|---|---|
| | F68 | IND | Mannitol | L-leucine[a] |
| F68 | 52.1 | | | |
| Indomethacin | | 159.9 | | |
| Mannitol | | | 165.7 | |
| L-leucine | | | | 273.8 |
| L-leucine:mannitol PM[b] | | | 165.6 | 235.0 |
| Indomethacin NS[c] | 45.9 | 146.3 | | |
| AFR 100-3 | – | 139.3 | 162.6 | 228.4 |
| AFR 160-3 | – | 149.5 | 162.4 | 222.8 |

[a] sublimation point, not melting point

[b] physical mixture of mannitol and L-leucine

[c] F68 stabilized indomethacin nanosuspension

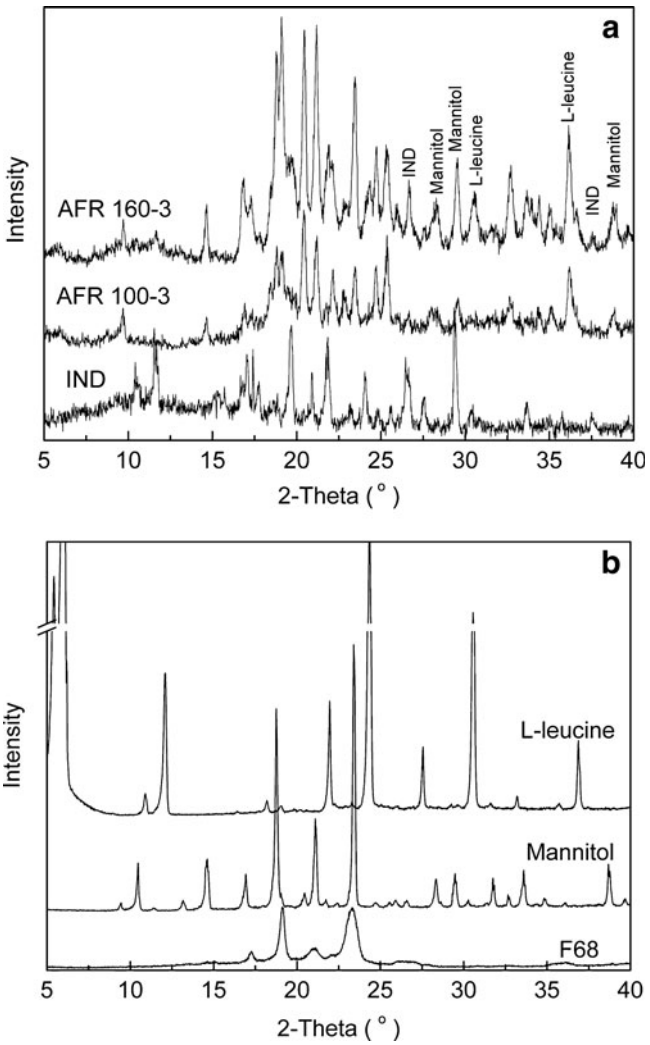


**Fig. 4** XRPD analyses of (**a**) bulk indomethacin and aerosol dried samples, and (**b**) F68, mannitol, and L-leucine. Labels in (**a**) show some of the peaks in the dried aerosol samples corresponding to crystalline starting materials.

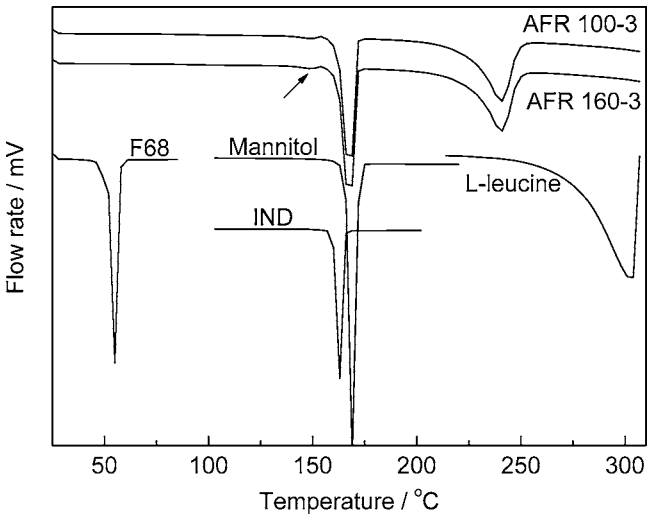


**Fig. 5** The DSC thermograms of F68, bulk indomethacin, mannitol, L-leucine and aerosol dried samples. The *arrow* indicates the small indomethacin peak in the aerosol dried samples.

points of mannitol in the AFR 100–3 and AFR 160–3 samples were only a few degrees less than the melting temperature of the bulk mannitol (165–169°C). These results, together with XRPD analysis, suggest that mannitol is in its original crystalline form. L-leucine crystals do not melt but sublime upon heating. In the AFR 100–3 and AFR 160–3 samples, the sublimation of L-leucine took place approximately 50°C lower than that of the bulk L-leucine. This is explained by its interactions with mannitol possibly via hydrogen bonding. The decrease in the sublimation temperature was also observed with a reference blend where L-leucine and mannitol were mechanically mixed in the same ratio as in the microparticles, which had an L-leucine sublimation peak at 235°C.

**Table III** The Size and Size Distribution of the Original Nanosuspension and Aerosol Dried Powders After Redispersion in Water. Sizes Are Taken From the Intensity Size Distribution Measured by Dynamic Light Scattering

| | Size (nm) | PI |
|---|---|---|
| Nanosuspensions | 485 | 0.51 |
| AFR 100-3 | 490 | 0.45 |
| AFR 160-3 | 1330 | 0.94 |

## Particle Composition

Fig. 6 shows the indomethacin loadings in the AFR 100–3 and AFR 160–3 samples and in fractionated particle sizes. Total drug amount of indomethacin in the AFR 100–3 sample was 8.7% (m/m) and in the AFR 160–3 sample 8.0% (m/m), which resulted in the encapsulation efficiencies of 63% and 58%, respectively. Although both samples had substantially the same total drug loadings, the AFR 100–3 had much lower drug amounts in the smaller size fractions (<422 nm), while AFR 160–3 tended to have higher drug amounts in the smaller size fractions (<241 nm). This could be explained as follows. As discussed above, the AFR 160–3 particles were exposed to 160°C for a short period of time to allow the sublimation of L-leucine at the particle surface. In addition to L-leucine sublimation, indomethacin nanocrystals partially melted. In the cooling step where L-leucine was deposited on particle surfaces, the fraction of melt indomethacin re-crystallized, forming very thin strips protruding from the particles. These can be seen in the TEM (Fig. 3c) and SEM images (Fig. 2h). In the gas-phase of the aerosol reactor, these crystalline strips have fragmented when the particles collided themselves and to the reactor walls. The fragments of the smallest sizes are

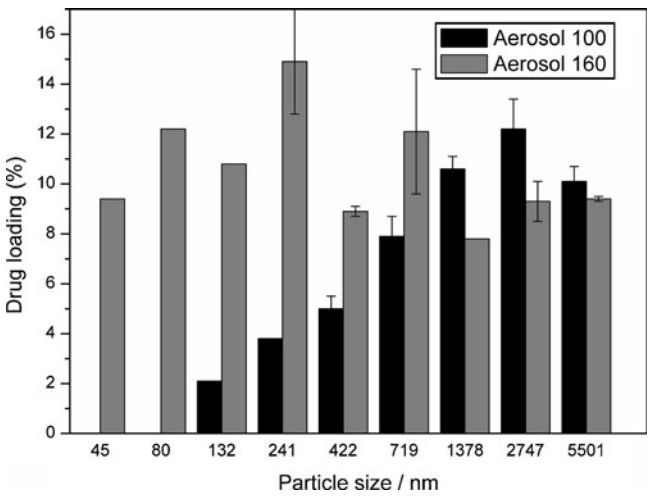


**Fig. 6** Indomethacin loadings (w-%) in the microparticles of different sizes ($n = 1–3$).

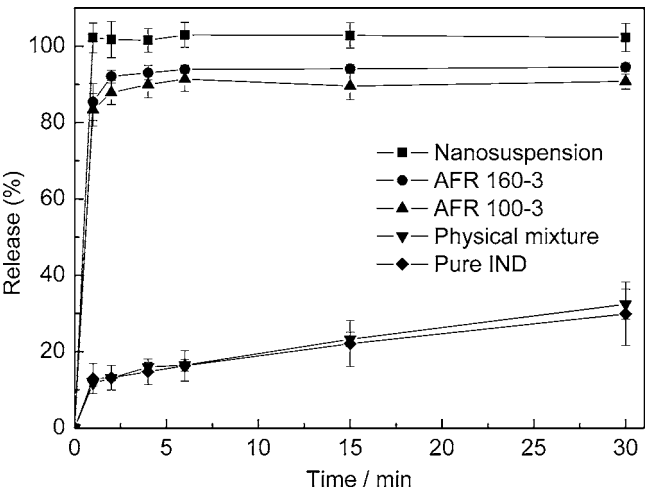


**Fig. 7** The dissolution profiles of aerosol dried samples, indomethacin nanosuspension, physical mixtures and pure indomethacin. The physical mixture was bulk indomethacin (75 w-%) and F68 (25 w-%).

expected to be responsible for high drug contents at small particle sizes, thus distorting the distribution in the impactor collection. In the AFR 100–3 sample, the lower size fractions did not contain indomethacin, since the drug nanoparticles were intact and had an average size larger than 400 nm. Thus, they cannot be collected in the smaller size fractions at all, even if not incorporated into microparticles. The amounts in the lower size fractions are due to the relatively broad size distribution of the original indomethacin nanosuspensions, which contains some amount of very small particles as well.

### Redispersion and Dissolution of Aerosol Particles

The AFR 100–3 sample re-dispersed well in water, resulting in a suspension where the particle size was the same as in the original nanosuspensions, ca. 500 nm (Table III). However, the particles in the AFR 160–3 sample aggregated to some extent, which resulted in larger suspended particles with relatively broad size distribution. It is hypothesized that the AFR 160–3 particles agglomerated during the collection when the re-crystallizing indomethacin formed 'bridges' and 'necks' between the particles.

Both the original indomethacin nanosuspension and AFR 100–3 and AFR 160–3 samples substantially improved the dissolution of indomethacin when compared to bulk indomethacin (Fig. 7). Indomethacin was dissolved completely from both aerosol samples and the original nanosuspension in less than 3 min. Thus, although the AFR 160–3 particles had aggregated and formed bigger particles, this did not affect the dissolution rate. The slightly slower initial dissolution (the first 2 min) of the drug from the aerosol samples is due to the dissolution of the microparticle structure, *i.e.* the L-leucine coating and mannitol matrix. This two-stage dissolution profile is in agreement with an earlier study where primary nanoparticles were prepared by a microprecipitation–homogenization process and encapsulated into 10–40 μm particles by spray-drying (31). Improved dissolution of indomethacin from the AFR100-3 and AFR 160–3 samples was solely due to the nanosize of indomethacin crystals and not to interaction between F68 and indomethacin. This was evident according to the dissolution of indomethacin from the physical mixture with F68, which had nearly identical dissolution rate as bulk indomethacin.

## CONCLUSIONS

In conclusion, we prepared successfully particle assemblies where nano-sized crystalline drug domains were embedded in solid microparticles. Indomethacin nanoparticles, which were prepared by media milling, were encapsulated in a mannitol matrix in the micron-sized particles coated with L-leucine using an aerosol flow reactor process. The stable solid particles were able to hold an intact crystalline form of indomethacin in the primary nanoparticles and to rapidly release the nanoparticles for fast dissolution of indomethacin. A soluble matrix is needed to disperse the drug nanoparticles and protect them against sintering and aggregation in the AFR, and leucine coating is needed to prevent the larger carrier particles from sintering. The process is also very much temperature dependent, and this must be selected based on the melting points of all the components in the system. This was outlined by the poorer morphology of the AFR 160–3 sample compared to AFR 100–3. Although the morphology did not reflect on the dissolution rate, redispersion studies showed that the primary nanoparticles did not survive the higher processing temperature. The AFR 100–3 particles would be suitable for further processing and, after size fractionation, also suitable for lung deposition studies. The present work is a promising approach towards a "nanos-in-micros" concept as a tool for pharmaceutical nanoparticle processing and novel drug delivery platforms. It could facilitate easier industrial use of drug nanocrystals, either as a step between nanosuspensions and tablet formulations or as a method for fabricating fast-dissolving particles for pulmonary drug delivery.

## ACKNOWLEDGMENTS

JR, AR, and EK acknowledge support from the Academy of Finland (project no. 133407).

## REFERENCES

1. Rabinow BE. Nanosuspensions in drug delivery. Nature Rev Drug Discov. 2004;3:785–96.
2. Müller RH, Keck CM. Challenges and solutions for the delivery of biotech drugs—a review of drug nanocrystal technology and lipid nanoparticles. J Biotechnol. 2004;113:151–70.
3. Peltonen L, Hirvonen J. Pharmaceutical nanocrystals by nanomilling; critical process parameters, particle fracturing and stabilization methods. J Pharm Pharmacol. 2010;62:1569–79.
4. Urata C, Yamauchi Y, Aoyama Y, Imasu J, Todoroki S-I, Sakka Y, *et al.* Fabrication of hierarchically porous spherical particles by assembling mesoporous silica nanoparticles via spray drying. J Nanosci Nanotechnol. 2008;8:3101–5.
5. Gómez-Gaete C, Fattal E, Silva L, Besnard M, Tsapis N. Dexamethasone acetate encapsulation into Trojan particles. J Control Release. 2008;128:41–9.
6. Grenha A, Seijo B, Remuñán-López C. Microencapsulated chitosan nanoparticles for lung protein delivery. Eur J Pharm Sci. 2005;25:427–37.
7. Mizoe T, Ozeki T, Okada HJ. Preparation of drug nanoparticle-containing microparticles using a 4-fluid nozzle spray drier for oral, pulmonary, and injection dosage forms. J Control Release. 2007;122(1):10–5.

8. El-Gendy N, Gorman EM, Munson EJ, Berkland C. Budesonide nanoparticle agglomerates as dry powder aerosols with rapid dissolution. J Pharm Sci. 2009;98:2731–46.
9. Kaye RS, Purewal TS, Alpar HO. Simultaneously manufactured nano-in-micro (SIMANIM) particles for dry-powder modified-release delivery of antibodies. J Pharm Sci. 2009;98:4055–68.
10. Kho K, Cheow WS, Lie RH, Hadinoto K. Aqueous re-dispersibility of spray-dried antibiotic-loaded polycaprolactone nanoparticle aggregates for inhaled anti-biofilm therapy. Powder Technol. 2010;203:432–9.
11. Grenha A, Seijo B, Serra C, Remuñán-López C. Chitosan-nanoparticle loaded mannitol microspheres: structure and surface characterization. Biomacromolecules. 2007;8:2072–9.
12. Lind A, von Hohenesche CF, Smått J-H, Lindén M, Unger KK. Spherical silica agglomerates possessing hierarchical porosity prepared by spray drying of MCM-41 and MCM-48 nanospheres. Microporous Mesoporous Mater. 2003;66:219–27.
13. Eerikäinen H, Peltonen L, Raula J, Kauppinen EI, Hirvonen J. Nanoparticles containing ketoprofen and acrylic polymers prepared by an aerosol flow reactor method. AAPS PharmSciTech. 2004;5:article 68.
14. Tong HHY, Shekunov BY, York P, Chow AHL. Influence of polymorphism on the surface energetics of salmeterol xinafoate crystallized from supercritical fluids. Pharm Res. 2002;19:640–8.
15. Eerikäinen H, Watanabe W, Kauppinen EI, Ahonen PP. Aerosol flow reactor method for synthesis of drug nanoparticles. Eur J Pharm Biopharm. 2003;55:357–60.
16. Lucas P, Anderson K, Potter UJ, Staniforth JN. Enhancement of small particle size dry powder aerosol formulations using an ultra low density additive. Pharm Res. 1999;16:1643–7.
17. Raula J, Kurkela JA, Brown DP, Kauppinen EI. Study of the dispersion behaviour of L-leucine containing microparticles synthesized with an aerosol flow reactor method. Powder Technol. 2007;177:125–32.
18. Raula J, Lähde A, Kauppinen EI. Aerosolization behavior of carrier-free L-leucine coated salbutamol sulphate powders. Int J Pharm. 2009;365:18–25.
19. Raula J, Thielmann F, Naderi M, Lehto V-P, Kauppinen EI. Influence on particle surface characteristics *vs.* dispersion behaviour of L-leucine coated carrier-free inhalable powders. Int J Pharm. 2010;385:79–85.
20. Raula J, Lähde A, Kauppinen EI. A novel gas phase method for the combined synthesis and coating of pharmaceutical particles. Pharm Res. 2008;25:242–5.
21. Lähde A, Raula J, Kauppinen EI. Simultaneous synthesis and coating of salbutamol sulphate nanoparticles with L-leucine in the gas phase. Int J Pharm. 2008;358:256–62.
22. Raula J, Thielmann F, Kansikas J, Hietala S, Annala M, Seppälä J, *et al.* Investigations on the humidity-induced transformations of salbutamol sulphate particles coated with L-leucine. Pharm Res. 2008;25:2250–61.
23. Raula J, Kuivanen A, Lähde A, Kauppinen EI. Gas-phase synthesis of L-leucine-coated micrometer-sized salbutamol sulphate and sodium chloride particles. Powder Technol. 2008;187:289–97.
24. Raula J, Kauppinen EI, Huck D, Kippax P, Virden A. Characterizing carrier-free DPI formulations: using laser diffraction and morphological imaging to examine aerosolization performance of carrier-free inhalation powders. Inhalation. 2010;4(4):8–11.
25. Paajanen M, Katainen J, Raula J, Kauppinen EI, Lahtinen J. Direct evidence on reduced adhesion of salbutamol sulphate particles due to L-leucine coating. Powder Technol. 2009;192:6–11.
26. Liu P, Rong X, Hirvonen J, Laaksonen T, Peltonen L. Nanosuspension of poorly soluble drugs: preparation and development by wet milling. Int J Pharm. 2011. 10.1016/j.ijpharm.2011.03.050.
27. Hillamo R, Kauppinen EI. On the performance of the Berner low pressure impactor. Aerosol Sci Tech. 1991;14:33–47.
28. Leroueil-Le Verger M, Fluckiger L, Kim Y-I, Hoffman M, Maincent P. Preparation and characterization of nanoparticles containing an antihypertensive agent. Eur J Pharm Biopharm. 1998;46:137–43.
29. Raula J, Kuivanen A, Lähde A, Jiang H, Antopolsky M, Kansikas J, *et al.* Synthesis of L-leucine nanoparticles via physical vapor deposition under various saturation conditions. J Aerosol Sci. 2007;38:1172–84.
30. Savolainen M, Heinz A, Strachan C, Gordond KC, Yliruusi J, Rades T, *et al.* Screening for differences in the amorphous state of indomethacin using multivariate visualization. Eur J Pharm Sci. 2007;30:113–23.
31. Chaubal MV, Popescu C. Conversion of nanosuspensions into dry powders by spray drying: a case study. Pharm Res. 2008;25:2302–8.